Energy Proceedings
Vol 29, 2022
ISSN 2004-2965

Comparison study of the pre-cooled and internally cooled liquid desiccant systems with different working fluids

Xiaosong cheng[1,2*], Thomas Meyer [2], Cristina Ricart [2], Meinard Gimm[2], Felix Ziegler[2], Yonggao Yin [1]

1 School of Energy and Environment, Southeast University, Nanjing 210096, China

2 Technische Universität Berlin, Institut für Energietechnik, Sekretariat KT 2, Marchstraße 18, 10587 Berlin, Germany

ABSTRACT

In this paper, a simulation is carried out on a pre-cooled liquid desiccant system working with aqueous Lithium Chloride (LiCl). The effects of different ambient air humidity on the outlet air humidities of absorber and desorber, crystallization of LiCl, cooling capacity, and COP of the system are analyzed. Besides, the system is compared to experimental results of an internally cooled liquid desiccant system using a new ionic liquid which is referred to as IL9. The conditions for both, the experiment as well as for the simulation are the same in terms of heat and mass transfer area, air inlet parameters, heat exchanger effectiveness, and hot and cooling water temperature. Some conclusions are summarized, for instance, the system using LiCl should be driven by the hot water of no more than 80℃ to avoid the crystallization risk, and the internally cooled system using IL9 shows a higher dehumidification performance than the pre-cooled system using LiCl especially at increased inlet air humidities.

Keywords: Pre-cooled liquid desiccant system, internally cooled, lithium chloride, ionic liquid, crystallization, dehumidification.

NONMENCLATURE

Latin letters	
C_p	specific heat capacity, KJ/(kg·K)
d_e	hydraulic diameter of packing, m
dx	the height of the microelement, m
dz	the length of the microelement, m
D_a	mass diffusivity of air, m^2/s
h_a	specific enthalpy of air, kJ/kg
h_c	heat transfer coefficient, KJ/(m^2·K)
h_d	mass transfer coefficient, kg/(m^2·s)
h_s	specific enthalpy of solution, kJ/kg; the calculating equation can refer to the reference[1]
H	height of packing, m
$\triangle H_{vap}$	heat vaporization of water vapor, kJ/kg
L	thickness of packing, m
$\dot{m}$	mass flow rate, kg/s
Sh	Sherwood number
W	width of structured packing
Greek symbols	
α	specific surface area of structured packing, 450m^2/m^3
ρ_a	air density, kg/m^3
ω_a	absolute humidity of air, kg/kg
ω_e	equilibrium absolute humidity on the desiccant surface which calculated by the surface vapor pressure, kg/kg
Subscripts	
a	air
abs	absorber
c	cooling
des	desorber
h	hot
in	inlet
out	outlet
s	liquid desiccant solution
w	water

1. INTRODUCTION

Thermally-driven liquid desiccant dehumidification technology removes the water vapor from air based on the vapor pressure difference between an air stream and a solution surface. The system can be divided into the pre-cooled and the internally cooled system according to at which stage the heat of absorption is rejected to the cooling water. In the absorber of the pre-cooled liquid desiccant system, the heat is transferred to the solution firstly and then released into the cooling water in the solution cooler. In contrast, in the absorber of the internally cooled system, the heat is taken away by cooling water during the absorption process. An analog configuration applies for the desorber.

A lot of research was carried out on the two systems and their components [2-5]. The working pair used in these studies are mainly inorganic desiccants, for instance, lithium bromide and lithium chloride, which have corrosion problems. Besides, the crystallization risk also very high for relative high driving temperature, and

it is usually not considered. In recent years, ionic liquids with non-corrosive and non-crystalline characteristics have attracted more and more researchers[6-8], especially used in the internally cooled system[9, 10]. Most of the research is concentrated on the study of a single liquid desiccant system. Besides, Varela et al.[9] compared the experimental dehumidification performance of a new internally cooled system using an ionic liquid solution with the simulated dehumidification performance of a pre-cooled system using LiCl solution at the different solution mass fluxes. The result shows the internally cooled system has better dehumidification performance. However, the results are limited since the comparison is not conducted for varying ambient conditions such as inlet air humidity which is a critical parameter. In addition, the crystallization limit of the LiCl system is not revealed in their comparison.

In this paper, the simulation of the pre-cooled liquid desiccant system using lithium chloride varying with the increasing ambient air humidity is studied, and the crystallization is also considered. After that, these simulation data are compared to experimental results which have been conducted at Technische Universität Berlin similar as described in [10]. These experiments are conducted using a new ionic liquid 9 (IL9), and the comparison between the two systems with the two different desiccants is analyzed.

2. PRE-COOLED LIQUID DESICCANT SYSTEM

2.1 System introduction

Fig.1 shows the schematic diagram of a pre-cooled liquid desiccant system. The main components of this system include absorber, desorber and heat exchangers. In the absorber, the solution flows from top to bottom due to gravity while the air cross flow in the horizontal direction. Meanwhile, the heat and mass transfer occur between liquid and air. The water vapor will transfer to the solution if the vapor pressure of air is larger than the equilibrium pressure of solution. At the same time, the heat of absorption is released into the solution results in the temperature rise and, thus, worsening the dehumidification performance of the absorber. For this kind of absorber, a higher solution flow rate should be set to dampen the liquid temperature rise. The weak solution from packing flows out to the tank and is mixed with strong solution (state 5) from the desorber. 70% of the solution at state 1 is pumped into the solution cooler to reach appropriate temperature (state 3) and then flows into the absorber. Similarly, 30% of the solution at state 1 is pumped into the desorber solution tank after heated by the heat exchanger to recover some heat from the hot strong solution coming from the desorber. The heat and mass transfer process in the desorber is similar to that in the absorber. The strong solution that has been pumped to the desorber has a higher equilibrium vapor pressure after heated by the solution heater and release the water vapor to the air caused by the pressure difference. The vapor releasing process will lead to a temperature drop due to the heat of desorption that is needed to evaporate the water out of the solution. Similar to the absorption process, a higher solution flow rate also needs to dampen the temperature decease of solution. 30% of the concentrated solution is pumped to the absorber tank after cooling down by the solution heat exchanger to complete the solution cycle of the whole system.

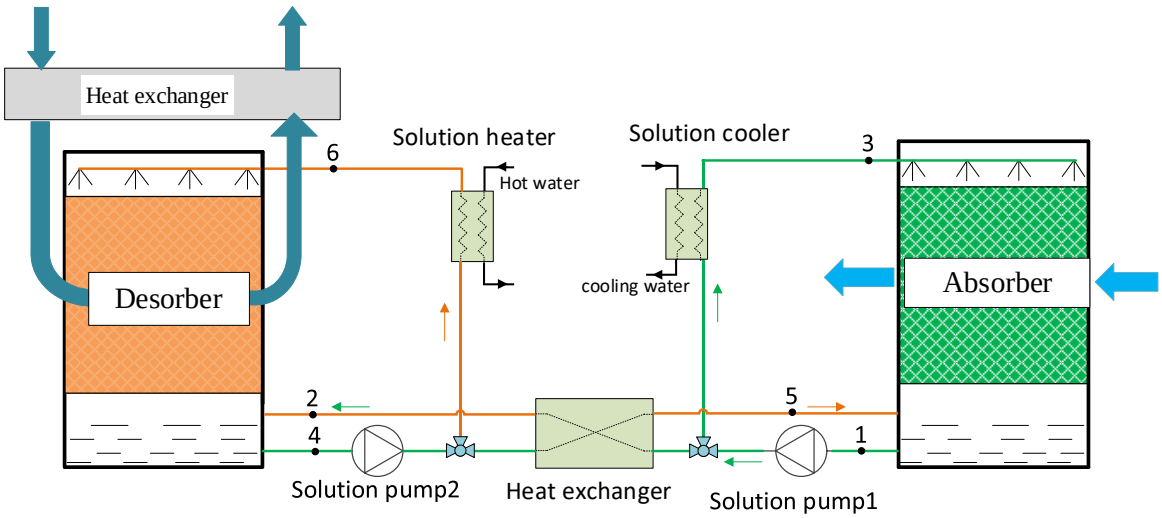

Fig.1 Schematic diagram of pre-cooled packed liquid desiccant system

2.2 *Mathematical model*

2.2.1 *Mathematical model of packing*

As shown in Fig. 2(a), the solution and air are cross flow in the packing. Since the solution and air are uniforms along the y-direction. A two-dimensional mathematic

model is built on the x-z plane which is discretized into M×N meshes shown in Fig.2(b). The heat and mass transfer between air and solution occur in every mesh shown in Fig.2(c).

The model assumptions are listed: (1) both the heat and mass transfer area are equal to the surface area of the packing; (2) the heat and mass transfer coefficients are uniform in the module; (3) the heat conduction and mass diffusion of air, and solution along with their flow directions are neglected; (4) the parameters vary only with their flow directions.

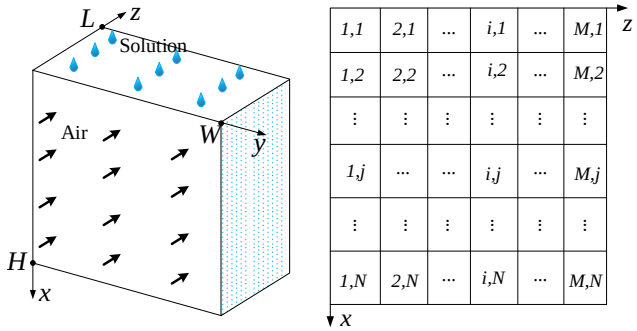

(a) Packing (b) A two-dimensional mesh

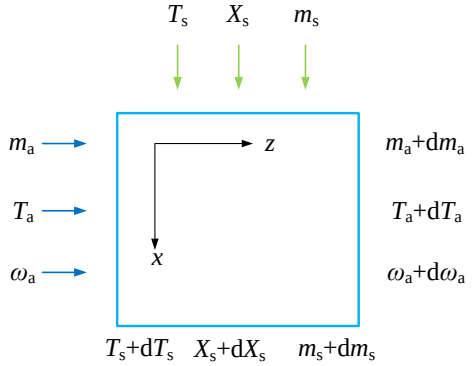

(c) Parameters varying in the microelement

Fig.2. Schematic of the differential process of packing

The control equations in every mesh are expressed as follows:

Mass conservation of water:

$$\dot{m}_a \cdot d\omega_a + d\dot{m}_s = 0 \quad (1)$$

Mass conservation of salt:

$$d(\dot{m}_s \cdot X_s) = 0 \quad (2)$$

Energy conservation of air and solution:

$$\dot{m}_a \cdot dh_a + d(\dot{m}_s \cdot h_s) = 0 \quad (3)$$

Heat transfer between air and solution:

$$\dot{m}_a \cdot C_{pa} \cdot dT_a = h_c \cdot (T_s - T_a) \cdot \alpha \cdot W \cdot dx \cdot dz \quad (4)$$

Mass transfer between air and solution:

$$\dot{m}_a \cdot d\omega_a = h_d \cdot (\omega_e - \omega_a) \cdot \alpha \cdot W \cdot dx \cdot dz \quad (5)$$

The boundary conditions are:

$T_s=T_{s,in}$, $X_s=X_{s,in}$ at x=0

$T_a=T_{a,in}$, $\omega_a=\omega_{a,in}$ at z=0

Equations (1~5) are discretized by using forward differential. The concrete calculation procedures of the whole packing are: (1) Calculate the outlet parameters of air and solution for the mesh (1,1) using the inlet boundary conditions; (2) Calculate the outlet air and solution parameters for the mesh (2,1) using the outlet parameters of mesh (1,1); (3) use the same method in the procedure (2) to calculate outlet parameters for the mesh (3,1), and until mesh(M,1); (4) use the solution outlet parameters of mesh (1,1) to (M,1) and air boundary conditions to calculate the outlet parameters of mesh (1,2) to (M,2), and then the same method is performed on meshes(1,3) to (M,3) until meshes (1, N) to (M, N).

The mesh size is M=500, N=300. The outlet parameters of the whole packing are the average outlet parameters of the last row meshes. Grid dependency on the results has been checked and the higher independent grid resolution have been applied here.

2.2.2 *Calculation of mass transfer coefficient*

The mass transfer coefficient between air and solution can be calculated by the Sherwood number, The formula is listed below:

$$h_d = \frac{Sh \cdot D_a \cdot \rho_a}{d_e} \quad (6)$$

The calculation equations can be provided by the reference [11], which has the same type of packing. For the absorber, the equation is expressed as:

$$Sh = 2.0\times10^{-3}\,\mathrm{Re}_a^{1.24}\,Sc_a^{0.33}\left(\frac{\dot{m}_{s,in}}{\dot{m}_{a,in}}\right)^{0.36}(1-X_{s,in})^{-1.28} \quad (7)$$

Besides, for the desorber, the equation is given as follow:

$$Sh = 5.55\times10^{-3}\,\mathrm{Re}_a^{0.994}\,Sc_a^{0.33}\left(\frac{\dot{m}_{s,in}}{\dot{m}_{a,in}}\right)^{0.101}(1-X_{s,in})^{-1.084}\left(\frac{T_{a,in}+273.15}{T_{s,in}+273.15}\right)^{2.05} \quad (8)$$

According to the experiment data in the literature [11], and the conditions in this simulation. The heat transfer coefficients are set as constant value, 30W/(m2·K) for the absorber and 10W/(m2·K) for the desorber.

2.2.3 *Mathematical model of heat exchanger*

For the solution-solution heat exchanger, solution-water heat exchanger, and air-air heat exchanger. The effectiveness model is used to calculate the outlet temperature. The effectiveness equation can be expressed as:

$$\varepsilon = \frac{\dot{m}_{cold}C_{p,cold}(T_{cold,out}-T_{cold,in})}{\min\{\dot{m}_{hot}C_{p,hot},\,\dot{m}_{cold}C_{p,cold}\}\cdot(T_{hot,in}-T_{cold,in})} \quad (9)$$

The outlet temperature of the cold fluid can be calculated by the effectiveness equation. The outlet temperature of the hot fluid can be calculated by the

energy conservation equations of the two fluids. The effectiveness of the liquid heat exchanger is 0.75 and 0.6 for the air heat exchanger. The effectiveness is derived from the experimental measurements in [10, 12].

2.2.4 Solution *mixing* process

In the absorber solution tank, the outlet solution from packing will mix with the solution from the desorber tank. The mixed solution concentration and enthalpy can be calculated by the following equations:

$$X_{\mathrm{s,abs,mix}} = \frac{\dot{m}_{\mathrm{s,abs,out}} X_{\mathrm{s,abs,out}} + \dot{m}_{\mathrm{s,des,mix}} (1-r_{\mathrm{des}}) X_{\mathrm{s,abs,mix}}}{\dot{m}_{\mathrm{s,abs,out}} + \dot{m}_{\mathrm{s,des,mix}} (1-r_{\mathrm{des}})} \tag{10}$$

$$h_{\mathrm{s,abs,mix}} = \frac{\dot{m}_{\mathrm{s,abs,out}} h_{\mathrm{s,abs,out}} + \dot{m}_{\mathrm{s,des,mix}} (1-r_{\mathrm{des}}) h_{\mathrm{s,abs,mix}}}{\dot{m}_{\mathrm{s,abs,out}} + \dot{m}_{\mathrm{s,des,mix}} (1-r_{\mathrm{des}})} \tag{11}$$

The solution temperature in the tank can be calculated by the concentration and enthalpy. The analogous equations could be written for the desorber also.

2.2.5 *Performance index*

The performance index of this system can be defined as the ratio of heat benefit from dehumidified air to heat consumption from hot water, the equation can be expressed as follow:

$$COP = \frac{\dot{Q}_{air}}{\dot{Q}_{input}} \tag{12}$$

There are different COP include sensible COP, latent COP and total COP which depends on the kind of benefit heat. The calculation equations for the benefit heat from dehumidified air in the absorber are given as follow:

$$\dot{Q}_{\mathrm{air,sensible}} = \dot{m}_{\mathrm{a}} (C_{\mathrm{pa,in}} T_{\mathrm{a,in}} - C_{\mathrm{pa,out}} T_{\mathrm{a,out}}) \tag{13}$$

$$\dot{Q}_{\mathrm{air,latent}} = \dot{m}_{\mathrm{a}} (w_{\mathrm{a,in}} - w_{\mathrm{a,out}}) \Delta H_{\mathrm{vap}} \tag{14}$$

The total benefit heat is the sum of the sensible load and latent load of dehumidified air. The input heat can be calculated by Eq. (15).

2.2.6 Mathematic model validation

Since there is no complete experiment data for the whole pre-cooled liquid desiccant system as shown in Fig 1., the validation can only be done for the most critical components-the absorber and desorber. For the simulation the inlet solution and air parameters, and packing size are set to the values provided in [13, 14] to calculate the outlet parameters. Then these simulated data is compared to the experimental data on temperature and humidity of the outlet air from the experimental data from [13, 14] shown in Fig.3. with almost every data in the range of below 10% deviation.

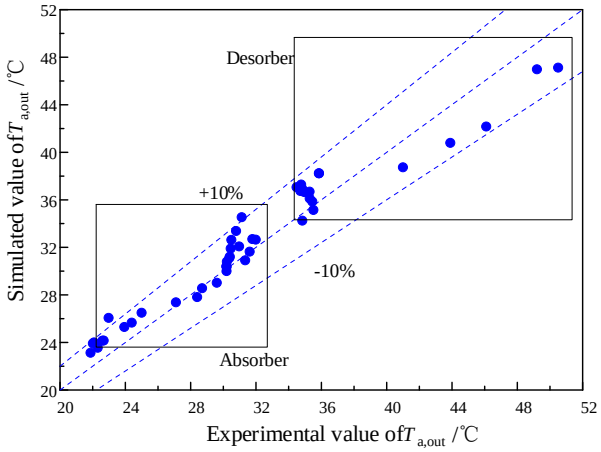

(a) Temperature comparison

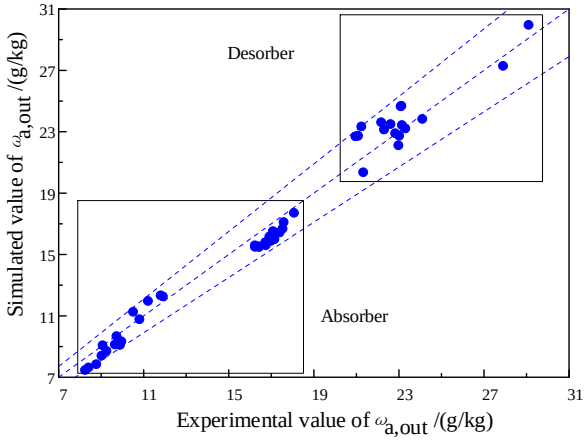

(b) Humidity comparison

Fig.3 comparison between simulation and measurement data

2.3 System simulation flowchart

The flow chart for this simulation is shown in Fig.4, the procedure mainly consisted of:

1) Input initial parameters, including the inlet water temperature, air parameters, the size of the packings, mass flow rate of air, and effectiveness of the heat exchanger.

2)Initializing some internal starting parameters, including the inlet concentration of absorber and desorber, solution temperature of absorber and desorber tanks

3) Calculate the absorber, desorber, and different heat exchangers in order, the calculation methods are already given in every model sections. Then obtaining the outlet parameters of fluids.

4) Calculate the air side dehumidified water vapor of absorber and desorber, and the new inlet solution concentration of absorber using the water mass imbalance information.

5) Judge whether dehumidified water vapor in the absorber and desorber satisfied the system error

requirement. Update the inlet solution concentration of absorber until the error meet the requirement.

6) After finishing the system iteration. Calculate the crystallization temperature using the inlet solution concentration of the absorber and comparing it with the simulated inlet solution temperature of the absorber, then output the crystallization information.

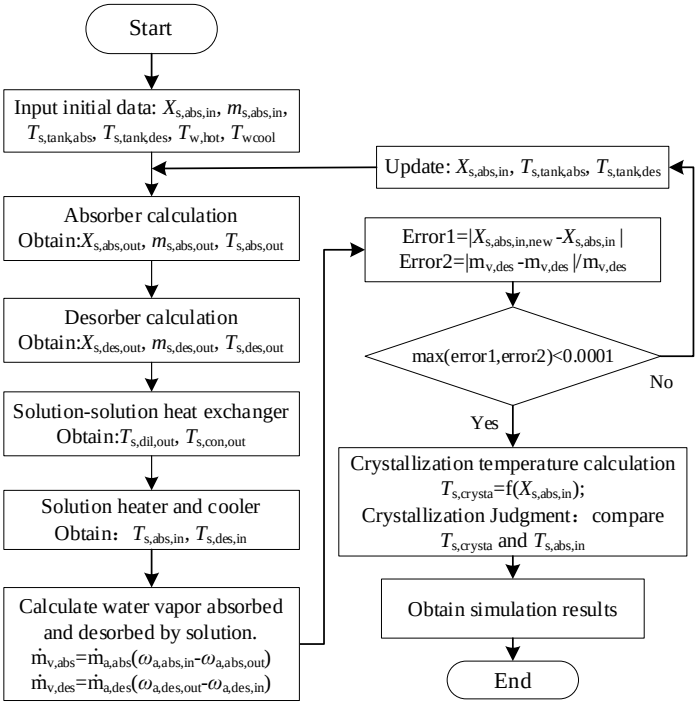

Fig.4 Simulation flow chart

2.4 Energy and mass conservation of system

There are four streams includes the dehumidified air, humidified air, cooling water and hot water transfer the energy with the system shown in Fig.5. The enthalpy flow of the streams can be expressed as follows:

$$\Delta\dot{H}_{w,h}=\dot{m}_{w,h}(h_{w,h,out}-h_{w,h,in}) \quad (15)$$

$$\Delta\dot{H}_{air,abs}=\dot{m}_{a,abs,in}(h_{a,abs,out}-h_{a,abs,in}) \quad (16)$$

$$\Delta\dot{H}_{w,c}=\dot{m}_{w,c}(h_{w,c,out}-h_{w,c,in}) \quad (17)$$

$$\Delta\dot{H}_{air,des}=\dot{m}_{a,des,in}(h_{a,des,out}-h_{a,des,in}) \quad (18)$$

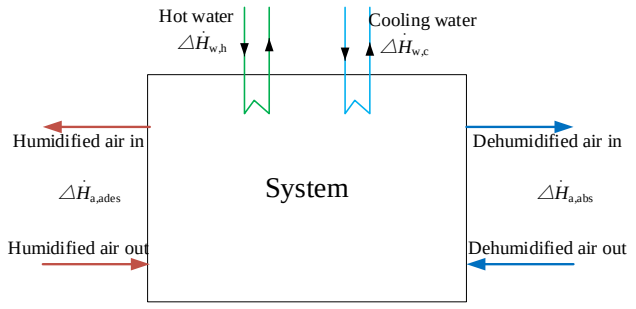

Fig.5 Enthalpy flow of pre-cooled system

The energy conservation error can be expressed as:

$$E_{balance}=\left|\frac{\Delta\dot{H}_{w,h}+\Delta\dot{H}_{air,abs}+\Delta\dot{H}_{w,c}+\Delta\dot{H}_{air,des}}{\Delta\dot{H}_{w,h}+\Delta\dot{H}_{air,abs}}\right| \quad (19)$$

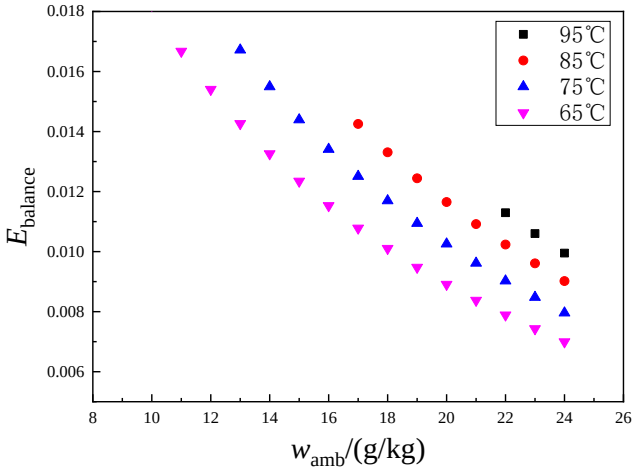

Fig.6 Energy balance of whole system

The energy conservation result is shown in Fig.6, the overall system energy balance error is lower than 1.8% for all the simulated points.

The water mass conservation of the system is that the water mass dehumidified to the solution in the absorber is equal to the water humidified to the air in the desorber. The calculation of water mass can be expressed as:

$$\dot{m}_{v,abs}=\dot{m}_{s,abs,out}(1-X_{s,abs,out})-\dot{m}_{s,abs,in}(1-X_{s,abs,in}) \quad (20)$$

$$\dot{m}_{v,des}=\dot{m}_{s,des,in}(1-X_{s,des,in})-\dot{m}_{s,des,out}(1-X_{s,des,out}) \quad (21)$$

Overall system water mass balance is given as follow:

$$M_{balance}=\frac{|\dot{m}_{v,abs}-\dot{m}_{v,des}|}{\dot{m}_{v,abs}} \quad (22)$$

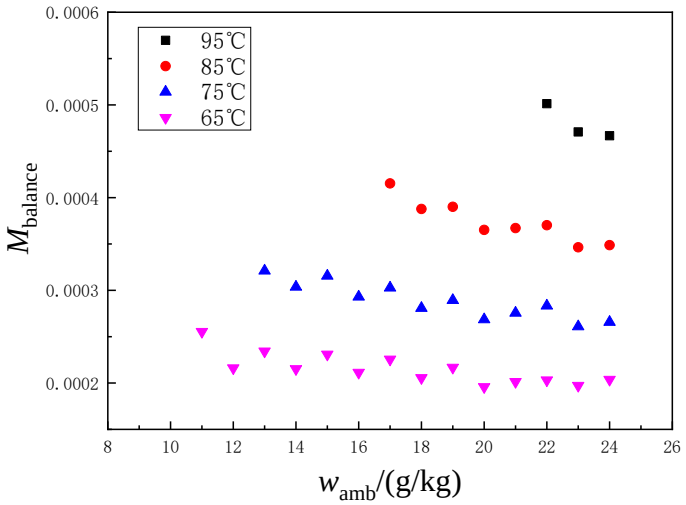

Fig.7 Mass balance of whole system

As is shown in Fig.7. The overall system water mass balance is low than 0.05%.

3. INTERNALLY COOLED LIQUID DESICCANT SYSTEM

The schematic diagram of internally cooled liquid desiccant system is shown in Fig.7. In this system, the cooling water and hot water join the heat and mass transfer process between air and solution directly. For instance, in the absorber, the cooling water can take away the released heat of absorption directly while the solution absorbed the water vapor from air. Hence the solution flow rate is much lower than that of pre-cooled system. The outlet solution of absorber is sent to the desorber after being pre-heated by the solution heat exchanger, similar as on the desorber side, the outlet solution is sent to the inlet of absorber after being cooled down by the solution heat exchanger. In the desorber side, the air heat exchanger is used to recover sensible heat from outlet humidified air to decrease the heat consumption.

The experiment research for this system using IL9 was carried out. More detailed information about this test rig can refer to the literatures but using a different ionic liquid 4 [10, 12].

The experimental conditions for internally cooled system, and simulation condition for pre-cooled system are shown in Table 1, which include the common conditions and some individual conditions for both two system.

.

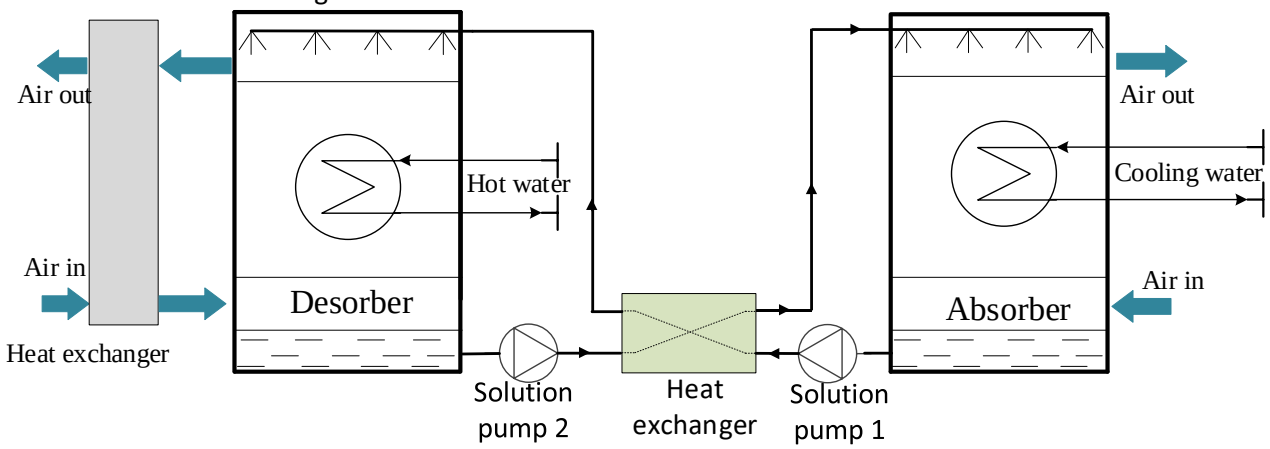

Fig.7 Schematic diagram of internally cooled liquid desiccant system

Table.1 Simulation and experiment conditions of two systems.

Common parameter	Dimension
Heat and mass transfer area of absorber/desorber	6.2m^2
Air flow rate	453kg/h
Velocity of air	1.2m/s
Cooling water temperature	30℃
Ambient air temperature	28℃
Liquid heat exchanger effectiveness	0.75
Air heat exchanger effectiveness	0.6
Individual parameter for pre-cooled system	**Dimension**
Packing size	L*W*H=0.32m *0.32m*0.14m
Solution flow rate	544 kg/h
Driving temperature	65~95℃
Individual parameter for internally cooled system	**Dimension**
Solution flow rate	155 kg/h
Driving temperature	85℃

4. RESULTS

4.1 *Simulation* results of pre-cooled system

As can be seen in Fig.7, the outlet humidity almost changes linearly with the inlet humidity. This is due to the linear variation of the vapor pressure difference between air stream and solution surface, and the almost constant heat and mass transfer coefficient. When the ambient humidity is fixed, the outlet humidity decreases as the driving temperature increases. That is because the higher driving temperature increases the concentration of solution and thus decreases the vapor pressure of solution surface. Hence lower humidities at the outlet of the absorber are achieved. When the humidity is low and the driving temperature is high, the solution crystallizes more likely. For instance, when the driving temperature is at 95℃, and the ambient humidity is lower than 20g/kg the solution will crystallize, but for 65℃, the ambient humidity can be lower than 10g/kg without crystallization. Therefore, considering the air condition and solution crystallization, the working pair LiCl is not suitable for the higher driving temperature. The reasonable range is from 60~80 ℃ for this given

system， which matches the conclusion in reference [15].

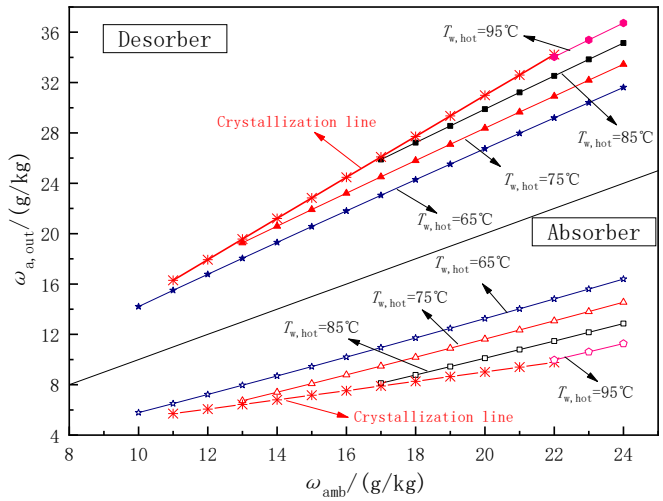

Fig.8. Outlet air humidity of the absorber and desorber

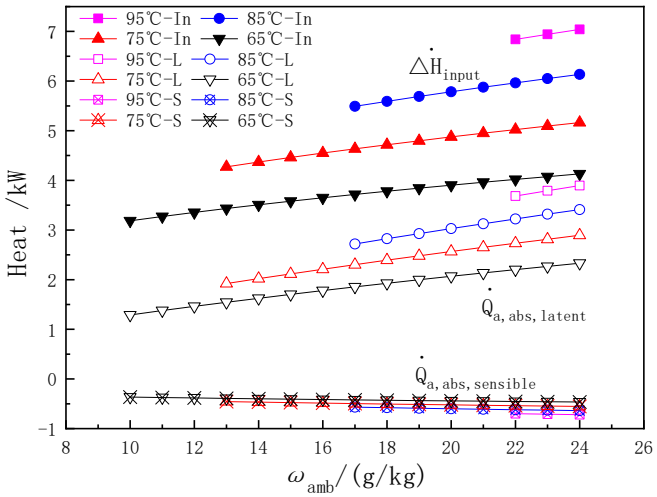

Fig.9. Cooling capacity and heat consumption

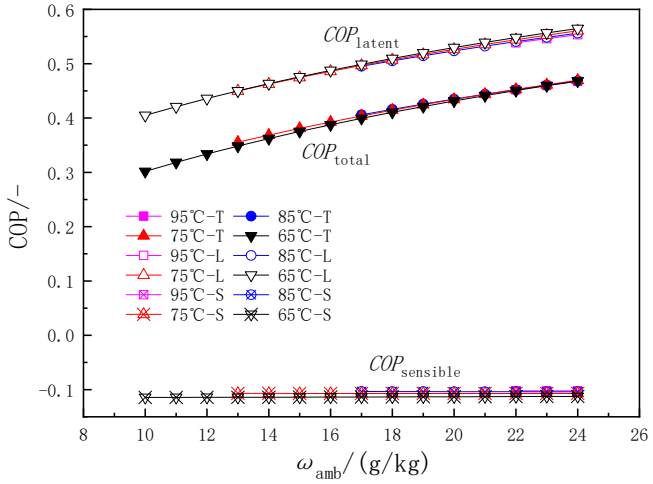

Fig.10. COP of system

As is shown in Fig.9, the latent load of dehumidified air in the absorber increased with the ambient humidity. The input heat from hot water has the same varying trend as the latent load of dehumidified air. The sensible load of dehumidified air in the absorber changes small compared to the latent load. From the figure 9, as the humidity is 22g/kg, the driving temperature is 85℃, the sensible load is -0.62kW, which is -10.4% of input heat, and the latent load is 3.3kW which is 54.0% of input heat. The total COP is only 43.6% because of the negative effect of sensible load in the absorber. Fig.10 describes the system COP influenced by the ambient air humidity and driving temperature. The latent COP increases as the humidity increases. That is due to the increased dehumidification rate, which results in more vapor humidified transfers to the air in the desorber. At the same time, the proportion of humidified air latent load in total input heat increased. Hence the latent COP is increased. The latent load of dehumidified air increases with the driving temperature. That is because the increasing solution concentration results in lower vapor pressure on the solution surface which increases the dehumidification rate owing to the rising vapor pressure difference. The latent COP changes very little owing to more heat input for higher driving temperatures.

4.2 Comparison of pre-cooled and internally cooled systems

The comparison of the simulation results of the pre-cooled liquid desiccant system using LiCl solution and the experiment results of the internally cooled liquid desiccant system using IL9 is shown in Fig.11. The driving temperature is 85℃, and the mean uncertainty for experiment data of outlet humidity in the absorber is 0.68g/kg and 1.25g/kg for the desorber, which are already shown in the figure. The outlet humidity of dehumidified air in the absorber increases for both of the two systems with inlet ambient air humidity, but the internally cooled system with IL9 has lower outlet humidity, and the IL9 can work normally even when the humidity is lower the crystallization line. As the ambient humidity increases, the humidity difference between the two systems increases. The phenomenon is mainly because the cooling water in the internally cooled system can take away the heat of absorption immediately resulting in a lower solution temperature than that of the pre-cooled system. When the ambient humidity is 22g/kg, the outlet humidity for the pre-cooled system is 11.5g/kg, while that of the internally cooled system is about 9g/kg, which is 2.5g/kg lower than the pre-cooled system. That means under the same heat and mass transfer area condition, the internally cooled system with IL9 has higher dehumidification potential.

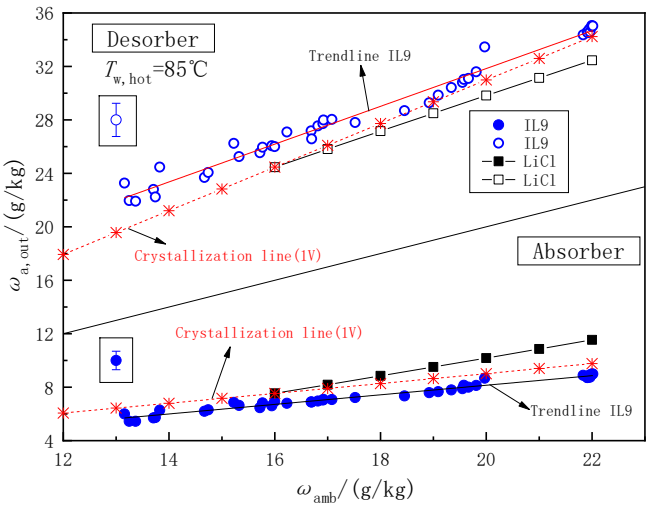

Fig.11. Comparison of two system

5. CONCLUSIONS

In this paper, a pre-cooled liquid desiccant dehumidification system using LiCl solution is simulated and compared with an internally cooled system using a new IL9 solution. Some conclusions are summarized as follows:

1)For the LiCl solution, the driving temperature should be no more than 80 ℃ to avoid the crystallization.

2) Because of temperature rise of dehumidified air, the sensible heat has a negative effect on the system performance, hence lower sensible heat will benefit the total system COP for both pre-cooled and internally cooled system.

3) The internally cooled liquid desiccant system with IL9 can dehumidify more water vapor from ambient air compare to pre-cooled system with LiCl, especially performs better at high humidity.

4) Higher driving temperature can achieve lower outlet humidity of the desorber. But it is not a good way to increase COP by increasing driving temperature since heat losses increase also.

ACKNOWLEDGEMENT

This research was supported by China Scholarship Council, the Evonik Industries AG.

REFERENCE

[1] Chaudhari SK, Patil KR. Thermodynamic Properties of Aqueous Solutions of Lithium Chloride. Physics and Chemistry of Liquids. 2002;40:317-25.

[2] Liu X, Jiang Y, Xia J, Chang X. Analytical solutions of coupled heat and mass transfer processes in liquid desiccant air dehumidifier/regenerator. Energy Conversion and Management. 2007;48:2221-32.

[3] Yin Y, Zhang X, Wang G, Luo L. Experimental study on a new internally cooled/heated dehumidifier/regenerator of liquid desiccant systems. International Journal of Refrigeration-Revue Internationale Du Froid. 2008;31:857-66.

[4] Yin Y, Zhang X, Peng D, Li X. Model validation and case study on internally cooled/heated dehumidifier/regenerator of liquid desiccant systems. International Journal of Thermal Sciences. 2009;48:1664-71.

[5] Gommed K, Grossman G. Experimental investigation of a liquid desiccant system for solar cooling and dehumidification. Solar Energy. 2007;81:131-8.

[6] Luo Y, Shao S, Xu H, Tian C. Dehumidification performance of [EMIM]BF4. Applied Thermal Engineering. 2011;31:2772-7.

[7] Watanabe H, Komura T, Matsumoto R, Ito K, Nakayama H, Nokami T, et al. Design of ionic liquids as liquid desiccant for an air conditioning system. Green Energy & Environment. 2019;4:139-45.

[8] Wang L, Liu X, Qu M, Liu X, Bahar B. An experimental study on dehumidification and regeneration performance of a new nonporous membrane-based heat and mass exchanger using an ionic liquid desiccant. Energy and Buildings. 2022;254.

[9] Varela RJ, Giannetti N, Saito K, Wang X, Nakayama H. Experimental performance of a three-fluid desiccant contactor using a novel ionic liquid. Applied Thermal Engineering. 2022;210.

[10] Zegenhagen MT, Ricart C, Meyer T, Kühn R, Ziegler F. Experimental Investigation of A Liquid Desiccant System for Air Dehumidification Working With Ionic Liquids. Energy Procedia. 2015;70:544-51.

[11] Peng D. Study of Combined Heat and Mass Transfer Characteristic and Performance on Solar Liquid Regenerator. Southeast University. 2009.

[12] Ricart C, Meyer T, Niemann K, Kühn R, Ziegler F. Investigation of a liquid desiccant system for air dehumidification working with an ionic liquid in a two-stage refrigeration system for cold stores. Processes of Refrigerants. 2015.

[13] Liu XH, Yi XQ, Jiang Y. Mass transfer performance comparison of two commonly used liquid desiccants: LiBr and LiCl aqueous solutions. Energy Conversion and Management. 2011;52:180-90.

[14] Shan N, Yin Y, Zhang X. Study on performance of a novel energy-efficient heat pump system using liquid desiccant. Applied Energy. 2018;219:325-37.

[15] Yin Y, Zhang X, Chen Z. Experimental study on dehumidifier and regenerator of liquid desiccant cooling air conditioning system. Building and Environment. 2007;42:2505-11.